

STORMS OR COLD FRONTS? WHICH ONE IS REALLY RESPONSIBLE FOR THE EXTREME WAVES REGIME IN THE COLOMBIAN CARIBBEAN COAST?

L. J. Otero¹, J. C. Ortiz-Royero¹, Julie K. Ruiz-Merchan¹, A. E. Higgins¹ and S. A. Henriquez¹

[1] Applied Physics Group – Ocean and Atmosphere Area – Physics Department, Universidad del Norte, Barranquilla, Colombia.

Correspondence to: L. J. Otero (ljotero@uninorte.edu.co)

Abstract

On Friday, March 7, 2009, a 200-meter-long section of the tourist pier in Puerto Colombia collapsed under the impact of the waves generated by a cold front in the area. The aim of this study is to determine the contribution and importance of cold fronts and storms on extreme waves in different areas of the Colombian Caribbean to determine the degree of the threat posed by the flood processes to which these coastal populations are exposed, and the actions to which coastal engineering constructions should be subject. In the calculation of maritime constructions, the most important parameter is the wave's height; therefore, it is necessary to definitively know the design wave height to which a coastal engineering structure should be resistant. This wave height varies according to the return period considered. Using Gumbel's extreme value methodology, the significant height values for the study area were calculated. The methodology was evaluated using data from the reanalysis of the spectral NOAA Wavewatch III (WW3) model for 15 points along the 1,600 km of the Colombia Caribbean coast (continental and insular) for the years 1979 to 2009. The results demonstrated that the extreme waves caused by tropical cyclones and cold fronts have different effects along the Colombian Caribbean coast. Storms and hurricanes are of greater importance in the Guajira Peninsula (Alta Guajira). In the central area formed by Baja Guajira, Santa Marta, Barranquilla, and Cartagena, the strong influence of cold fronts on extreme

1 waves is evident. On the other hand, in the southern region of the Colombian Caribbean coast,
2 from the Gulf of Morrosquillo to the Gulf of Urabá, even though extreme values of wave heights
3 are lower than in the latter regions, they are dominated mainly by the passage of cold fronts.
4 Extreme waves in the San Andrés and Providencia insular region present a different dynamic
5 from that in the continental area due to its geographic location. The wave heights in the extreme
6 regime are similar in magnitude to those found in Alta Guajira, but the extreme waves associated
7 with the passage of cold fronts in this region have lower return periods than the extreme waves
8 associated with hurricane season.

9 These results are of great importance when evaluating the threat of extreme wave height in the
10 coastal and port infrastructure. Both for purposes of the design of new constructions, and in the
11 coastal flood processes, due to run-up because, according to the site of interest in the coast, the
12 forces that shape extreme wave heights are not the same.

13 **Key words:** Gumbel's distribution function, hurricanes, extreme waves, Caribbean
14 Sea, cold fronts

15

16

17 **1 Introduction**

18 The principal source of coastal energy and responsible for sediment dynamics are waves. The
19 waves generated by 'sea'-type local winds and those generated offshore by atmospheric
20 disturbances known as swells determine the average and extreme maritime climate of a region.
21 The activities that develop in coastal or maritime areas, such as fishing, maritime transport and
22 transit, oil exploitation, structure design, and even surfing, demand knowledge of waves. The
23 maritime climate, particularly winds, is a dynamic phenomenon that presents short-period cyclic
24 variations (daily, weekly), seasonal variations, and long-term variations. Considering that winds
25 are the main wave-generating agent, the wave climate also varies based on this pattern. Given the
26 incidence of the wave climate in the operation and construction costs of maritime infrastructures,
27 it is important to design these constructions taking into account the temporal variation of this
28 phenomenon at an oceanic and local scale.

1 Cold fronts occur when two air masses at different temperatures and densities come into
2 proximity. The cold air mass with higher density pushes the hot air, making it ascend. The rising
3 hot air cools down, producing clouds, the pressure gradient in the area, strong winds, storms, and
4 increases in the wave height or swell through its passage along the Colombian Caribbean coast,
5 (Ortiz et al., 2013).

6 The incidence of cold fronts in the Colombian Caribbean coast has not been widely studied. Cold
7 fronts are noted in the marine-meteorological monthly reports of the Center of Oceanographic
8 and Hydrographic Research (Centro de Investigaciones Oceanográficas e Hidrográficas, CIOH)
9 of the General Maritime Direction (Dirección General Marítima, DIMAR). Their potential
10 incidence in the events of extreme waves in the region under study has been described by Ortiz et
11 al. (2014a), where the most important marine-meteorological event of the last 10 years in the
12 Colombian Caribbean was reconstructed, namely the passage of a cold front on March 2009
13 whose associated waves caused 200 meters of the pier at Puerto Colombia to collapse.

14 Ortiz et al. (2013) performed the characterization of cold fronts in the central region of the
15 Colombian Caribbean and their relation with extreme waves, finding that cold fronts have been
16 the cause of the major waves in this region over the last 15 years.

17 On the other hand, Ortiz (2012) and Ortiz et al. (2014b) described the threat of hurricanes in the
18 Colombian Caribbean. Joan in 1988 and Lenny in 1999 were two of the most important events in
19 the continental Caribbean coast, while for San Andrés Island, the list is longer: Hattie in 1961,
20 Alma in 1970, Joan in 1988, Cesar in 1996, Katrina in 1999, and Beta in 2005 are hurricanes that
21 have affected the island over the last 50 years. This is why the San Andrés y Providencia
22 Archipelago is the zone in the Colombian Caribbean that is most vulnerable to hurricane threats.

23 In this context, the traditional method of constructing the extreme wave regime has consisted of
24 performing predictions of waves based on historical information for a period of no less than 10
25 years (Martínez and Coria, 1993; Naveau et al., 2005). Based on this information, the most
26 unfavorable extreme values of each year are selected, and the results are then extrapolated to
27 different return periods.

28 Although there is no physical, theoretical, or empirical evidence of which should be the selection
29 or adjustment of a probability distribution function for the calculation of the design wave height,

1 the Gumbel or Fisher Tippet I and Weibull distribution functions are widely used for such
2 purposes, as reported by Martínez and Coria (1993), Katz et al. (2002), García et al. (2004), and
3 Naveau et al. (2005).

4 In response to the lack of information on the variability of extreme waves in coasts of the
5 Colombia Caribbean, the main objective of this study is to determine the importance and
6 contribution of cold fronts and storms for extreme waves to ascertain the actions to which coastal
7 and port structures in different regions of the Colombian Caribbean should be subjected and,
8 similarly, to assess the degree of the threat to which coastal populations are exposed due to flood
9 processes caused by wave run-up.

10 **2 DESCRIPTION OF THE STUDY AREA**

11 The coastline of the Colombian Caribbean has a wide territory that extends from 8°N to 13°N and
12 from the country's border with Panamá in the southwest (SW) at longitude 79°W to the Guajira
13 Peninsula on the northeast (NE) at longitude 71°W. The Colombian coastal area is approximately
14 1,600 km in length and includes important cities from the economic and touristic perspective:
15 Riohacha, Santa Marta, Barranquilla, and Cartagena. The total area of the Colombian Caribbean
16 is approximately 590,000 km². These cities are home to maritime and river ports of great
17 importance for the economy of the country. Of the four cities, the most populated one is
18 Barranquilla (2,400,000 inhabitants), followed by Cartagena (1,200,000 inhabitants), Santa Marta
19 (415,000 inhabitants), and Riohacha (150,000 inhabitants).

20 The insular Colombian Caribbean is formed by the Archipelago of San Andrés, Providencia,
21 Santa Catalina, the Roncador, Quitasueño, Serranía, and other cays, adjacent islets, and deep-
22 water coral reefs.

23 San Andrés Island is located in the Caribbean Sea, at 180 km east of Nicaragua and northeast of
24 Costa Rica and 480 km northwest of the Colombian coast (Parsons, 1954). The island of San
25 Andrés is the largest of the islands that form part of the Archipelago of San Andrés, Providencia,
26 and Santa Catalina, with a total extension of 26 km². It is surrounded on its northwestern side by
27 a small coral reef and several cays that are home to marine flora and fauna (Geister, 1973).

1 It is interesting to review and analyze the phenomenon responsible for the extreme wave regime
2 in this area because the entire region of the Colombian Caribbean is not located at the same
3 latitude.

4 The Colombian climate is characterized by two seasons in the year that are marked according to
5 precipitation: a dry season and a wet season. The main dry season in the region occurs from
6 December to May; in this season, swells produced by cold fronts can occur. The wet season
7 occurs the rest of the year, interrupted by a relative minimum in June and July known as Indian
8 summer (Andrade and Barton, 2001). The dry season and Indian summer are associated with the
9 jet stream winds of San Andrés and the northeastern (NE) trade winds. When the jet stream of
10 San Andrés is stronger, the dry season occurs in the entire Caribbean coast, coinciding with very
11 intense NE trade winds; the same occurs with Indian summer (Andrade and Barton, 2001). By
12 contrast, the wet season, which ranges from August to November, coincides with the time of
13 most intense jet stream winds from Chocó and less intense jet stream winds from San Andrés
14 (Poveda, 2004).

15 Along this entire region, the rainiest month of the year is October, and the driest months are
16 February and March. From December to March, the intertropical convergence zone (ITCZ) is
17 located over South America, the high pressure centers are strong in the Caribbean, and the
18 northeast trade winds are maximal, which is consistent with the main dry season in the Caribbean
19 region. From July to September, the location of the ITCZ shifts towards the center of the
20 Caribbean, trade winds weaken, and southwest (SW) winds, which are weaker but can bring
21 strong storms to the Caribbean region, dominate. These annual periods coincide with maximums
22 in the jet streams from San Andrés and Chocó, respectively. However, the second maximum jet
23 stream from San Andrés, which occurs from July to August and is associated with Indian
24 summer, is not directly related to the ITCZ but instead to a temporal intensification of the high
25 pressure system from the North Atlantic (Andrade and Barton, 2001).

26 Wiedeman (1973) and Kjerfve (1981) established that Caribbean tides are weak, with a tidal
27 range oscillating from 20 to 30 cm, and occasionally surpassing 50 cm; therefore, it was
28 classified as microtidal (range <2 m). Using information from different tide stations in the
29 Caribbean, Morales (2004) concluded that, in Cartagena and Islas Del Rosario, which are located
30 in the central Colombian Caribbean, the tide classification is mixed and mainly diurnal.

1 Similarly, the zone of the Santa Marta bay also located in central Colombian Caribbean has a
2 mixed tidal classification that is mainly diurnal and with a tidal range of 48 cm (García et al.,
3 2011), while the insular region of San Andrés is found within the mixed tidal classification and is
4 mainly semidiurnal.

5 The annual wave cycle presents a bi-modal behavior influenced by the NE trade winds, showing
6 2 wind periods, intense waves, and low precipitation in the dry season and 2 wind periods, weak
7 waves, and high precipitation during the wet season (Mesa, 2010).

8

9 **3 METHODOLOGY**

10 In the area under study, there are no extensive historical records of waves of an experimental
11 nature (Meza, 2010). Buoys of the National Oceanic and Atmospheric Administration (NOAA)
12 are very far from the coastal zone of the Colombian Caribbean. The DIMAR controls several
13 directional buoys near the Colombian coasts in the Caribbean and the Pacific. For the Caribbean,
14 the DIMAR has 2 buoys, 41193 and 41194, located near the coasts of Barranquilla and Riohacha,
15 respectively, and in the central Caribbean, the NOAA controls scalar buoy 42058, as shown in
16 Fig. 1.

17 The National Data Buoy Center (NDBC) database has records for 2008, 2009, and 2010.
18 Directional buoy 41194, which began operation in 2007, is located near Bocas de Ceniza, which
19 is the mouth of the Magdalena River in the Caribbean Sea, located near the city of Barranquilla.
20 Directional buoy 41193 is near Puerto Bolívar (Guajira Department) and has records since 2010,
21 and buoy 42058 has been collecting data since 2005. Therefore, in order to characterize the wave
22 climate, it is necessary to resort to data obtained from models, visual waves, or satellites
23 (Agudelo et al., 2005). According to Martínez and Coria (1993), for an analysis of extreme
24 waves, it is necessary to have at least 10 years of wave data in the area of interest. For this
25 purpose, a historic database of 30 years (1979-2009) from 15 reanalysis virtual buoys distributed
26 along the Caribbean coastline from the NCEP Climate Forecast System Reanalysis Winds
27 (CFSRR), was initially analyzed (Chawla et al., 2011). The Data was downloaded from web site:
28 http://polar.ncep.noaa.gov/waves/CFSR_hindcast.shtml. The spatial resolution of wave data for
29 the Caribbean Sea is $1/6^\circ \times 1/6^\circ$. The wave model used at NCEP is a third generation wind wave

1 model WAVEWATCH III (Tolman, 2009). The wind fields with which the model was forced
2 originate from a new reanalysis of the atmospheric, oceanic, sea-ice and land data from 1979
3 through 2010, and a reforecast run with this reanalysis (Saha et al., 2010). The detailed
4 description of the data is carried out in Chawla et al., (2013).

5 The locations of these virtual buoys (Bv) are shown in Fig. 2. Similarly, this figure shows the
6 segmentation of the continental and insular Colombian Caribbean coast into 4 zones, as proposed
7 by Ortiz (2012), in accordance with their level of vulnerability to the threat of hurricanes.

8 Given the limited information of oceanographic buoys in the area of study, detailed parametric
9 calibration and validation were applied to the re-analysis wave series for data coinciding with the
10 significant wave heights (H_s) in undefined depths for a zone in the Caribbean where data from
11 oceanographic buoys existed. In this study, the data from buoy 42058 was used for the calibration
12 of the database, and the data from buoy 41194 was used for validation. Buoy 42058 was selected
13 to perform the calibration process for two main reasons: first, due to the higher extension of
14 continuous data available and, second, due to its location in undefined depths.

15 From the data on significant wave heights (H_s) from the WW3 model for the point 14.9°N-75°W
16 and the data collected by oceanographic buoy 42058, a detailed parametric calibration method
17 was applied for coinciding data using power and linear regression models (Tomas, 2009). With
18 the coefficients obtained in each regression model, the data from the series corresponding to buoy
19 Bv05 were corrected. These data were validated with the values of significant wave heights (H_s)
20 measured by oceanographic buoy 41194 of Barranquilla, Colombia.

21 With the aim of verifying the degree of adjustment of the measured and calculated time series,
22 the D adjustment index and the Average Deviation P described by Willmott (1981) were
23 applied.,in order to determine the adjustment degree of the regression models, the r^2 correlation
24 coefficient was used.

25 In accordance with Wornon and Welsh (2002a, 2002b), the D index is very sensitive to errors in
26 the mean square root of the difference between predictive and observed values. A $D = 0$ shows
27 total dissociation, while $D = 1$ shows a perfect association between the measured and calculated
28 data. Willmott's D index is defined as:

$$D = 1 - \frac{\sum_{n=1}^N (Pn - On)^2}{\sum_{n=1}^N (|Pn - O| + |On - O|)^2} \quad (1)$$

where Pn is the prediction performed, On are the measurements, and O is the mean of the measurements performed.

The Average Deviation P is defined as:

$$bias(P) = \frac{\sum_{n=1}^N (Pn - On)^2}{\sum_{n=1}^N On} \quad (2)$$

For example, a deviation of -0.05 shows mean underestimations of the order of 5%.

To differentiate the influence of cold fronts on hurricanes, calculations of extreme values were performed for 2 seasons of the year: the hurricane season of the Caribbean from June to November and the cold front season from December to May.

For the calculation of extreme values, Gumbel's maximum distribution or Fisher-Tippet type I distribution were selected. This distribution is suitable for random, identically distributed, and independent variables and is widely used to characterize extreme regimes of oceanographic geophysical variables. Gumbel's maximum distribution is a bi-parametric function with a location parameter λ and a scale parameter δ , (García et al., 2004).

$$F(x) = e^{-e^{-b}} \quad (3)$$

where

$$b = \frac{x - u}{\alpha} \quad (4)$$

$$\alpha = \frac{S_x}{\lambda} \quad (5)$$

$$u = \bar{x} - \delta\alpha \quad (6)$$

x is the data series, S_x is the standard deviation, and \bar{x} the arithmetic mean of the data series. The values of λ and δ are selected according to the number of data, in this case, $\lambda = 0.53622$ and $\delta = 1.11237$.

1 From the series of annual maximums, the characteristic waves for return periods of 5, 10, 25,
2 50, and 100 years were calculated using Gumbel's maximum distribution.

3

4 **4 ANALYSIS AND RESULTS**

5 Fig.3 Shows the results of the calibration of the H_s WW3 re-analysis data and the data from the
6 Central Caribbean oceanographic buoy (42058). The lines represent the linear regression Eq. (7)
7 and power regression Eq. (8) models. The dispersion diagram shows that both models present a
8 good correlation with the data, with r^2 values of 0.92 and 0.93 for the power and linear regression
9 models, respectively. The calibration equations obtained were the following:

$$10 H_{scal} = \alpha H_{sbuoys} + \beta \quad (\alpha = 1.047 \pm 0.024; \beta = 0.07619 \pm 0.047) \quad (7)$$

$$11 H_{scal} = a H_{sbuoys}^b \quad (a = 1.096 \pm 0.0265; b = 0.9847 \pm 0.0284) \quad (8)$$

12 Based on the previous calibration relations, the H_s data from the WW3 model in the coordinate
13 point 11.25°N-74.75°W, coinciding with the location of buoy 41194, were corrected.

14 Fig. 4(a) compares the uncorrected H_s values of the WW3 model and the data from buoy 41194,
15 with a $D = 0.97$ and a $bias(P) = -0.06$. Figures 4(b) and 4(c) compare the H_s series from buoy
16 41194 with the H_s series corrected using a linear and power regression model, respectively.
17 Based on the adjustment index D and Willmott's Average Deviation P , the improvement in the
18 adjustment degree in the H_s time series are shown in Table 1. As shown in the table, the indices
19 show improvements of equal proportion for both models. In this sense, the linear regression
20 model was selected for the correction of the WW3 H_s series of the 15 points selected for the
21 analysis.

22 Once the information of the data for each of the 15 buoys was calibrated and validated, we
23 proceeded to perform a detailed analysis from which a total of 8 buoys were selected as
24 representative samples of each of the zones of interest based on the H_s value and the location of
25 the cities and ports of interest.

26 As noted above, tropical cyclones occur in the season from June to November, and cold fronts
27 occur from December to May. Therefore, the H_s time series of the 8 buoys were divided for these
28 2 seasons with the aim of independently performing extreme wave analysis. That is, the extreme

1 regime was calculated considering only the H_s information for the months between June and
2 November, and the extreme regime was also calculated taking into account only the months from
3 December to May. Additionally, the extreme regime was calculated considering the complete
4 series to identify which seasons of the year contributed the most to this regime. This method of
5 presenting the results allows a comparative analysis to identify in which seasons of the year the
6 most extreme waves for the area occur and also to establish which atmospheric phenomenon is
7 responsible for generating these extreme waves.

8 The results of the application of Gumbel's theory for the significant height H_s on each of the 8
9 buoys are shown in Figures 5, 8, 10, and 11 in the order in which the previous results were
10 presented.

11 Virtual buoys Bv01-Bv05 are located in the arid zone of the Alta Guajira, north of the Colombian
12 Caribbean (Zone 01 in Fig. 2.). The bar diagrams in Fig. 5 explicitly show that the height of
13 extreme waves is clearly influenced by tropical cyclones. During this period, the extreme waves
14 associated with return periods of 5 and 10 years, oscillate between 3.2 m and 4.5 m. For return
15 periods of 25, 50, and 100 years varying 5.5 m and 6.6 m in height. The highest waves for this
16 region occur because Alta Guajira is the closest zone to the trajectory of tropical cyclones passing
17 through the Colombian Caribbean (Ortiz, 2012). According to Rodríguez (2011), during this time
18 of the year, there is a higher probability of the passage of tropical waves from the east (known as
19 such due to their movement from east to west) that can evolve into tropical depressions, tropical
20 storms, and hurricanes.

21 On the other hand, the dry season of the year, from December to May, is influenced by the
22 increase of trade winds from the northeast (Bernal et al., 2006; Paramo et al., 2011) and the
23 passage of cold fronts coming from the northern hemisphere, producing strong tides (Ortiz et al.,
24 2013). Extreme wave heights for return periods of 5 and 10 years show significant heights that
25 oscillate between 3.0 m and 4.2 m. Meanwhile, the extreme waves for return periods of 25, 50,
26 and 100 years take significant height values that vary between 3.6 m and 4.8 m.

27 Regarding the waves' direction, it is considered that it is likely from E and ENE with heights
28 mainly between 1 m and 3 m.

1 When comparing the extreme regime for virtual buoys Bv01 and Bv03 located in the Alta Guajira
2 area, it can be observed that the significant heights, for return periods of 5 and 10 years that take
3 the complete series of annual maximums, show values greater than the significant heights
4 obtained when dividing the series by season. However, for a return period of more than 50 years,
5 the significant height extrapolated from the cyclone season data surpasses the significant height
6 obtained with the annual maximums. This occurs because, over the 30 years of the registry, there
7 were 16 years in which the maximum significant height was presented in hurricane season. These
8 values were the highest of the record (between 4.9 m and 5.2 m). In the remaining 14 years, the
9 maximum significant height in cyclone season is lower in comparison to the wave height
10 registered in the cold front season. This difference in the significant height for each period
11 generates a greater dispersion in the maximums of the season from June to November. The
12 difference in the standard deviation of data causes an increase in the slope of the line H_s against
13 the return period in the semi-logarithmic space (Fig. 6) of the model for the cyclone season. In
14 the remaining virtual buoys, there is no variation in the extreme regime when increasing the
15 return period because all of the extreme wave events are found to be related to 1 of the 2 seasons
16 is shown in Fig. 7.

17 The diagrams of Fig. 8, correspond to the central zone of the Colombian Caribbean formed by
18 Baja Guajira, Santa Marta, Barranquilla, and Cartagena (Zone 02 in Fig. 2). Because of the
19 geographic location of this zone in Colombia, it is important to highlight that the dry and wet
20 climate seasons present a significant variability in the duration and intensity of the winds and the
21 rain regime due to the influence of different events, such as the El Niño-South Oscillation event
22 (ENSO) on its warm phase (Niño) and on its cold phase (Niña), trade winds, the passage of
23 waves from the east, and cold fronts, among others (Nystuen et al., 1993; Andrade and Barton,
24 2001).

25 It can be seen that in Bv06, for both the cyclone season (June-November) and the cold front
26 season (December-May), there are similar magnitudes in the extreme waves, but they present
27 slightly higher values in the dry season, especially in the return periods of 5 and 25 years. From
28 Bv09, it can be seen that the most energetic waves in the coastal zone of this region are
29 influenced clearly by cold fronts. While the less energetic waves are dominated by tropical
30 cyclones. Therefore, the extreme waves for return periods of 5 and 10 years register significant

1 heights between 3.5 m and 4.5 m, and the extreme waves for return periods of 25, 50, and 100
2 years present values that vary between 4.0 m and 5.5 m in height,.

3 In this transition region, the behavior of extreme waves is modified because a clearer and
4 stronger preponderance of cold fronts begins, decreasing the influence of tropical storms on this
5 regime. This modification can clearly be seen in Fig. 8, where the extreme regime calculated
6 considering the complete series is influenced by the maximum wave heights that occur in the cold
7 front season.

8 It is important to highlight that the extreme wave height regime in an area of the central zone of
9 the Caribbean is higher than in Alta Guajira (i.e Buoy 09). This zone of the Colombian coast
10 ceases to be directly influenced by tropical cyclones and the extreme regime starts to prevail due
11 to the passage of cold fronts.

12 In relation to the direction of the waves, it is reported that, in this sector of the central Colombia
13 Caribbean, the NE direction is predominant with heights mainly between 1 m and 3 m. With
14 respect to zone 01, the energy in the average regime is similar, and the direction of the wave
15 trains is affected by the orientation of the coastline, which goes from NE to SW.

16 The data shown in Fig. 9, correspond to the zone known as the western Caribbean, which is
17 formed by the area between the Morrosquillo Gulf and the Urabá Gulf (Zone 03 in Fig. 2). In this
18 zone, regardless of the season, the wave energy is lower in comparison to the other zones of the
19 Colombian Caribbean because the Morrosquillo Gulf is protected from winds by Boquerón Island
20 and the other islands of San Bernardo, the Urabá Gulf is protected from waves in the eastern
21 zone, and the Colombia bay is protected by its closed-U shape. The northwestern coast of the gulf
22 directly receives waves originating from the open sea (Escobar, 2011). In this zone of the
23 Colombian Caribbean, few studies have been conducted on waves, especially on waves in the
24 Urabá Gulf.

25 The winds of this region also present bimodal characteristics with a predominance of strong
26 winds from the north and northeast in the dry season. In the wet season, winds from the south and
27 southeast predominate (Roldán, 2007). Oceanic-atmospheric factors such as winds and waves
28 present significant differences between the dry season (December-April) and wet season (the

1 remaining months), which in turn is in accordance with the displacement of the ITCZ (Meza et
2 al., 1997).

3 The bar diagrams on Fig 9 show that the least energetic waves of the entire Colombian coast,
4 which are mainly influenced by the passage of cold fronts, can be found in this area. The
5 significant height for return periods of 5 and 10 years show values oscillating between 4.0 m and
6 4.5 m, and the extreme waves for return periods of 25, 50, and 100 years take values that vary
7 between 4.5 m and 5.0 m in height. On the other hand, the least energetic extreme waves are
8 dominated by tropical cyclones. In these graphics, it is evident that the extreme wave height is
9 clearly influenced by cold fronts, which is confirmed when the values of the extreme wave
10 heights are calculated taking into account the complete series of maximum heights. Regarding the
11 waves' direction in the southwestern Colombian Caribbean sector, NE and NNE are
12 predominant, with heights mainly between 1 m and 2 m. Regarding zones 01 and 02, the energy
13 in the average regime is lower.

14 Bv15 is located in the insular region of San Andrés and Providencia (Zone 04 in Fig. 2). In Fig.
15 10 shows that extreme waves for return periods of 5 and 10 years have significant height values
16 between 5.0 m and 5.5 m for the wet season influenced by hurricanes, while for the dry season
17 influenced by cold fronts, the values oscillate between 4.5 m and 4.7 m. The extreme waves for
18 return periods of 25, 50, and 100 years take values that vary between 5.1 m and 5.7 m in height
19 for the dry season influences by cold fronts, while for the wet season, the values for extreme
20 values oscillate between 6.2 m and 7.0 m. Because of its geographic location out over the
21 Colombian Caribbean Sea, the islands of San Andrés and Providencia exhibit high vulnerability
22 to tropical storms and the passage of cold fronts (Ortiz et al., 2014b). Regardless of the analyzed
23 series, it is clearly evident that the waves generated by tropical storms are the waves that govern
24 the extreme regime. This is because the San Andrés and Providencia islands are located in a zone
25 where hurricanes pass.

26 Previous studies have revealed that, according to historical records for the years 1900 to 2013, a
27 total of 17 hurricanes have affected San Andrés and Providencia, and in 7 of these phenomena,
28 the eye of the storm was located less than 150 km from the islands. Of these 7 hurricanes, Joan in
29 1988 generated the highest wave heights, with significant height values of 5.0 m SE of the island
30 of San Andrés in the 50-meter isobath (Ortiz et al., 2014b). The position of Bv15 coincides with

1 the outline of the intermediate calculation grid employed by Ortiz et al. (2014b) (Fig. 11). It can
2 be seen that the maximal significant wave height generated by the passage of Joan in the outline
3 of the grid is 5.0 m. This value of H_s , according to Fig. 10, is associated with a return period of
4 25 years. It is important to highlight that, over the last 50 years, of all the hurricanes that have
5 affected the island of San Andrés, only Joan has generated wave heights of 7.8 m (Ortiz et al.,
6 2014b). Nevertheless, values higher than 5 m. have been registered during that season, due to the
7 passage of hurricanes. In the 30-year analysis of the dry season for Bv-15 heights superior than 5
8 m. were not found. This finding means that wave heights in the extreme regime associated with
9 the passage of tropical storms in Zone 04 have lower return periods than the wave heights
10 associated with the cold fronts season.

11 The wind speed patterns in the San Andrés and Providencia islands are influenced by fluctuations
12 in the Azores anticyclone, the latitudinal fluctuations of the ITCZ, the entrance of cold fronts, and
13 the passage of hurricanes in the zone.

14 The wide insular platform and coral reefs located along the northeast coast act as a natural
15 defense that dissipates the energy of waves before they reach the coast. The southwest coast is
16 completely exposed to the extreme waves' energy due to its narrow insular platform and scarce
17 coral reefs (Ortiz et al., 2014b).

18

19 **5 Conclusions**

20 The present study has permitted to conclude that extreme waves along the Colombian Caribbean
21 coasts (continental and insular) are not generated by the same forces. The geomorphology of the
22 1,600 kilometers of coastline of the Colombian Caribbean and its geographical position ensure
23 that the waves generated by extreme events do not have the same magnitude of influence in all
24 areas. There is a clear difference for the north zones (Alta Guajira), central zones (Baja Guajira,
25 Santa Marta, Barranquilla, and Cartagena), west zone (Morrosquillo Gulf and Urabá Gulf), and
26 the Archipelago of San Andrés because the waves' extreme regime is influenced by the spatial
27 and temporal changes of the atmospheric phenomena that develop over a particular zone in the
28 Colombian Caribbean coast, depending on the dry and wet climatic seasons.

1 Based on the analysis of the variability of extreme waves in the continental coast of the
2 Colombian Caribbean, it can be concluded that, in the higher part of the Guajira (Zone 01), there
3 are higher extreme wave heights caused by tropical cyclones, which is consistent with the
4 findings reported in Ortiz (2012), followed by the central zone (Zone 02), where the influence of
5 extreme waves is associated with the passage of cold fronts, while less energetic extreme waves
6 occur in the western part of the Caribbean (Zone 03), where they are mainly forced by the
7 passage of cold fronts.

8 The extreme waves in the insular region of San Andrés and Providencia (Zone 04) show a
9 dynamic different from the continental region due to its geographic location. Although the
10 waves' heights in the extreme regime are similar in magnitude to those found for Zone 01 (Alta
11 Guajira), the extreme waves associated with the passage of tropical storms in this zone have
12 lower return periods than the extreme waves associated with the cold fronts season.

13 The previous results make a valuable contribution to the moment of determining the extreme
14 regime and the design waves for the construction of coastal infrastructure. Furthermore, they
15 provide an important component for the planning of alert and mitigation strategies against
16 marine-meteorological threats. In addition, because different zones of the Colombian Caribbean
17 are affected by coastal erosion, this study constitutes a source of data for the further analysis of
18 how and how much these events are related to erosion.

19

20

21 **Acknowledgments**

22 The authors wish to express their gratitude to the Directorate of Research and Projects (Dirección
23 de Investigaciones y Proyectos (DIDI)) of the Universidad del Norte and to the Departamento
24 Administrativo de Ciencia y Tecnología e Innovación de Colombia (COLCIENCIAS) for their
25 support in conducting this research.

26

27

28

1 **References**

- 2 Agudelo, P., Restrepo, A., Molaes. A., Tejada. C., Torres. R., and Osorio, A.: Determinación del
3 clima medio y extremal en el Caribe Colombiano [Determination of the average and extreme
4 climate in the Colombian Caribbean]. *Boletín Científico CIOH.*, 23, 33-45, 2005.
- 5 Andrade, C. and Barton, E.: Eddy development and motion in the Caribbean Sea. *J. Geo. Res.*,
6 105, 26191-26201, 2001.
- 7 Bernal, G., Poveda, G., Roldán, P., and Andrade, C.: Patrones de variabilidad de las temperaturas
8 superficiales del mar en la Costa Caribe Colombiana [Variability patterns of the sea surface
9 temperatures in the Colombian Caribbean coast]. *Rev. Acad. Colomb. Cienc.*, 30(115), 195-208,
10 2006.
- 11 Chawla, A., Spindler, D., and Tolman, H.L.: A thirty year wave hindcast using the latest NCEP
12 Climate Forecast System Reanalysis winds. *Proc. 12th Int. Workshop on Wave Hindcasting and*
13 *Forecasting*, Waikoloa, HI, Environment Canada, 11, 2011.
- 14 Chawla, A., Spindler, D., and Tolman, H.L.: Validation of a thirty year wave hindcast using the
15 Climate Forecast System Reanalysis winds. *Ocean Modell.*, 70, 189–206, 2013.
- 16 Escobar, C.: Relevance of coastal processes on the hydrodynamics of The Gulf Of Urabá
17 (Colombian Caribbean Sea). *Boletín de Investigaciones Marinas y Costeras-INVEMAR.*, 40(2),
18 327-346, 2011.
- 19 García, F., Palacio, C., and Garcia, U.: Tide constituents at Santa Marta Bay
20 (Colombia). *Dyna.*, 78(167), 142-150, 2011.
- 21 García, V., Garcia-Bartual, R., Cabrera, E., Arregui, F., and García, J.: Stochastic Model to
22 Evaluate Residential Water Demands. *Journal of Water Planning and Management*, 130(5), 386-
23 394, 2004.
- 24 Geister, J.: Los arrecifes de la isla de San Andres (Mar Caribe, Colombia) [The coral reefs in the
25 island of San Andrés (Caribbean Sea, Colombia)]. *Mitt Inst. Colombo Alemán Invest. Cient.*, 7,
26 211-228, 1973.
- 27 Kjerfve., B.: Tides of the Caribbean Sea. *Journal of Geophysical Research*, 86, 4243-4247, 1981.

1 Martínez, A. and Coria, P.: Distribución de probabilidad de la altura del oleaje dentro de la bahía
2 de Todos los Santos, B.C. [Probability distribution of waves' height inside the Todos los Santos
3 Bay, B.C.], México. Ciencias Marinas, 19(002), 203-218, 1993.

4 Mesa, J. C.: Metodología para el reanálisis de series de oleaje para el caribe colombiano
5 [Methodology for the re-analysis of wave series for the Colombian Caribbean]. Tesis Doctoral,
6 Universidad Nacional de Colombia, Colombia, Medellin, 5-12, 2010.

7 Mesa, O., Poveda, G., and Carvajal, F.: Introducción al Clima de Colombia [Introduction to
8 Colombia's climate]. Illustrated, Universidad Nacional de Colombia, Medellín, Colombia, 390,
9 23-27, 1997.

10 Molares, R.: Clasificación e identificación de las componentes de marea del Caribe Colombiano
11 [Classification and identification of the components of the Colombian Caribbean tide], Boletín
12 científico CIOH., 22, 105-114, 2004.

13 Nystuen, J. and Andrade, C.: Tracking mesoscale ocean features in the Caribbean Sea using
14 Geosat altimetry. Journal of Geophysical Research: Oceans (1978–2012), 98(C5), 8389-8394,
15 1993.

16 Ortiz, J. C., Otero, L., Restrepo, J., Ruiz, J., and Cadena, M.: Cold fronts in the Colombian
17 Caribbean Sea and their relationship to extreme wave events. Natural Hazards and Earth System
18 Science, 13(11), 2797-2804, 2013.

19 Ortiz, J. C., Salcedo B., and Otero, L.: Investigating the collapse of the Puerto Colombia Pier
20 (Colombian Caribbean Coast) in March of 2009: methodology for the reconstruction of extreme
21 events and their impact on the coastal infrastructure. Journal of Coastal Research, 30(2), 291-300,
22 2014a.

23 Ortiz, J. C., Plazas, J. M., and Lizano, O.: Evaluation of Extreme Waves Associated with
24 Cyclonic Activity on San Andrés Island in the Caribbean Sea since 1900. Journal of Coastal
25 Research. In-Press. doi: <http://dx.doi.org/10.2112/JCOASTRES-D-14-00072.1>, 2014b.

26 Ortiz, J. C.: Exposure of the Colombian Caribbean Coast, including San Andrés Island, to
27 Tropical Storms and Hurricanes, 1900– 2010, Nat. Hazard J., 61, 815-827, 2012.

1 Naveau, P., Nogaj, M., Ammann, C., Yiou, P., Cooley, D., and Jomelli, V.: Statistical methods
2 for the analysis of climate extremes. *C R Geosci*, 337(10-11), 1013-1022, 2005.

3 Paramo, J., Correa, M., and Núñez, S.: Evidencias de desacople físico-biológico en el sistema de
4 surgencia en La Guajira, Caribe colombiano [Evidence of the physico-biological decoupling of
5 the upwelling system in La Guajira, Colombian Caribbean]. *Revista de biología marina y*
6 *oceanografía*, 46(3), 421-430, 2011.

7 Parsons, J. J.: English Speaking Settlement of the Western Caribbean, *Yearbook of the*
8 *Association of Pacific Coast Geographers*, 16, 3-16, 1954.

9 Poveda, G.: La hidroclimatología de Colombia: una síntesis desde la escala inter-decadal hasta la
10 escala diurna [The hydroclimatology of Colombia: a synthesis from the inter-decade scale to the
11 diurnal scale]. *Rev. Acad. Colomb. Cienc.*, 28(107), 201-222, 2004.

12 Katz, R. W., Parlange, M. B., and Naveau, P.: Statistics of extremes in hydrology *Adv Water*
13 *Resour*, 25, 1287-1304, 2002.

14 Rodríguez, L.: Identificación de zonas homogéneas en la interfase mar-aire del mar caribe
15 colombiano y relación entre la variabilidad de parámetros oceanicos y atmosféricos de algunos
16 puntos representativos de estas zonas y la oscilación atlántico norte [Identification of
17 homogeneous areas at the sea-air interphase of the Colombian Caribbean Sea and relation
18 between the variability of oceanic and atmospheric parameters of some representative points of
19 these zones and the North Atlantic Oscillation]. Tesis de maestria. Universidad Nacional de
20 Colombia, Columbia, Medellín, 35-40, 2011.

21 Roldán, P.: Modelamiento del patrón de circulación de la bahía Colombia, golfo de Urabá-
22 Implicaciones para el transporte de sedimentos [Modeling of the movement pattern of Colombia
23 Bay, Gulf of Urabá - Implications for sediment transport]. Tesis de Maestría, Universidad
24 Nacional de Colombia, Colombia, Medellín, 102, 2007.

25 Tomas, A.: Metodologías de calibración de bases de datos de reanálisis de clima marítimo
26 [Methodologies of the calibration of marine climate reanalysis database]. Tesis Doctoral,
27 Universidad de Cantabria., España, 69-89, 2010.

1 Saha, S., Moorthi, S., Pan, H. L., Wu, X., Wang, J., Nadiga, S., Tripp, P., Kistler, R., Woollen, J.,
2 Behringer, D., Liu, H., Stokes, D., Grumbine, R., Gayno, G., Wang, J., Hou, Y. T., Chuang, H.
3 Y., Juang, H. M. H., Sela, J., Iredell, M., Treadon, R., Kleist, D., Van Delst, P., Keyser, D.,
4 Derber, J., Ek, M., Meng, J., Wei, H., Yang, R., Lord, S., Van Den Dool, H., Kumar, A., Wang,
5 W., Long, C., Chelliah, M., Xue, Y., Huang, B., Schemm, J.-K., Ebisuzaki, W., Lin, R., Xie, P.,
6 Chen, M., Zhou, S., Higgins, W., Zou, C. Z., Liu, Q., Chen, Y., Han, Y., Cucurull, L., Reynolds,
7 R. W., Rutledge, G., and Goldberg, M.: The NCEP climate forecast system reanalysis. *Bull. Am.*
8 *Meteor. Soc.*, 91, 1015–1057, 2010.

9 Tolman, H. L.: User manual and system documentation of WAVEWATCH III version3.14. Tech.
10 Note 276, NOAA/NWS/NCEP/MMAB, 220 pp, 2009.

11 Wiedemann, H.: Reconnaissance of the Ciénaga Grande de Santa Marta, Colombia: physical
12 parameters and geological history. *Mitt. Inst. Colombo-Alemán Invest. Cient.*, 7, 85-119, 1973.

13 Willmott, C.: On the validation of models *Phys. Geog.*, 2, 183-194, 1981.

14 Wornon, S. and Welsh, D.: An MPI quasi time-accurate approach for nearshore wave prediction
15 using SWAN code. Part II. *Coastal Engineering Journal*, 44(3), 257-280, 2002b.

16 Wornon, S. and Welsh, D.: An MPI quasi time-accurate approach for nearshore wave prediction
17 using SWAN code. Part I. *Coastal Engineering Journal*, 44(3), 247-256, 2002a.

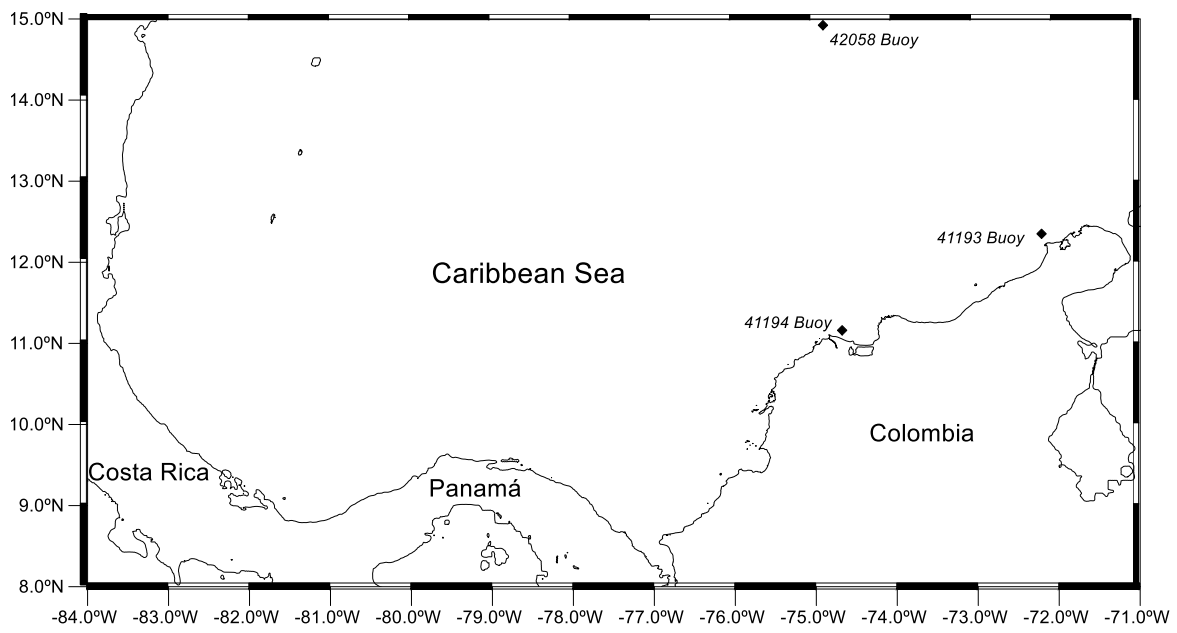
18

19

1 Table 1. Adjustment index D and Willmott's Average Deviation P , data from buoy 41194 and
 2 WW3 model.

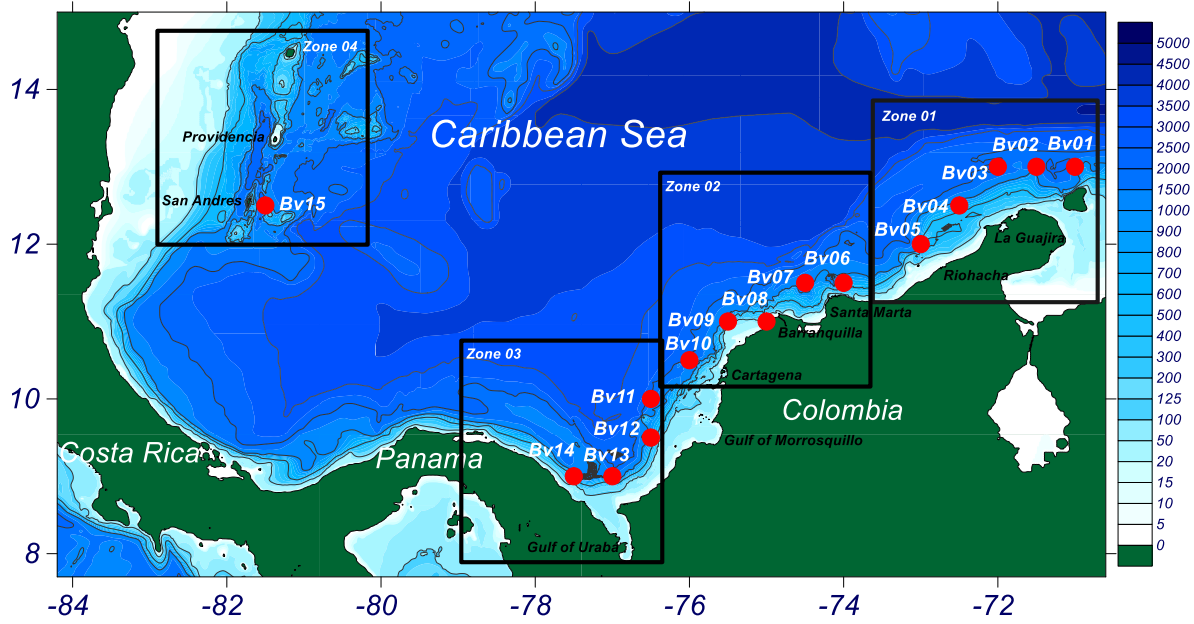
Significant Height $H_S(m)$	D	$Bias(P)$
WW3 vs Buoy (41194)	0.97	-0.06
WW3 corrected with linear regression vs Buoy (41194)	0.99	0.02
WW3 corrected with power regression vs Buoy (41194)	0.99	0.02

3
 4
 5
 6
 7
 8
 9
 10
 11



1
2 Figure 1. Location of the DIMAR and NOAA buoys on the Colombian Caribbean coast.

3
4
5
6
7



1

2

3

Figure 2. Location of the 15 virtual buoys generated using WW3 and the zoning proposed by Ortiz (2012) based on the threat degree of hurricanes.

5

6

7

8

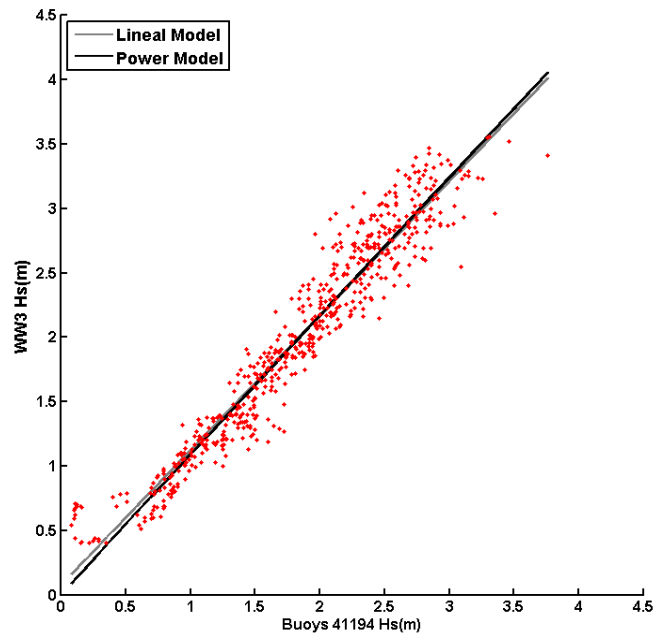
9

10

11

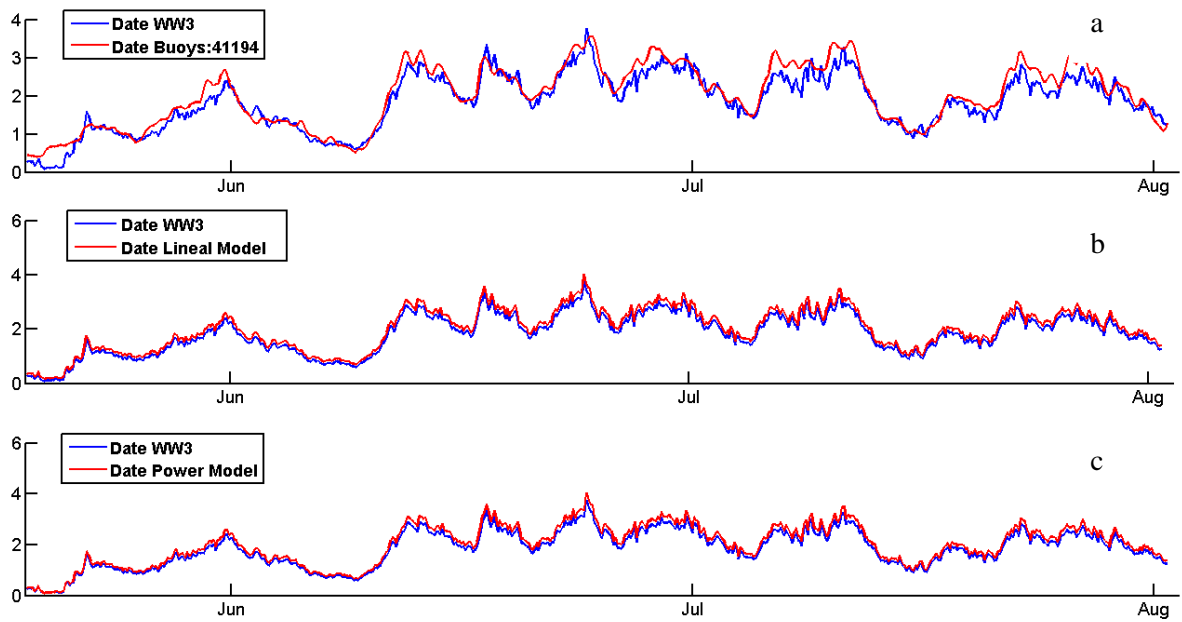
12

13



1
2
3
4
5
6
7
8
9
10
11
12

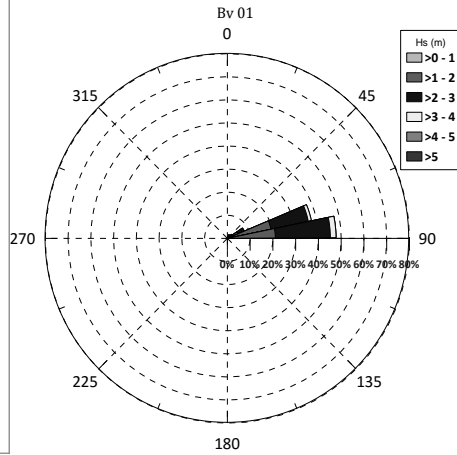
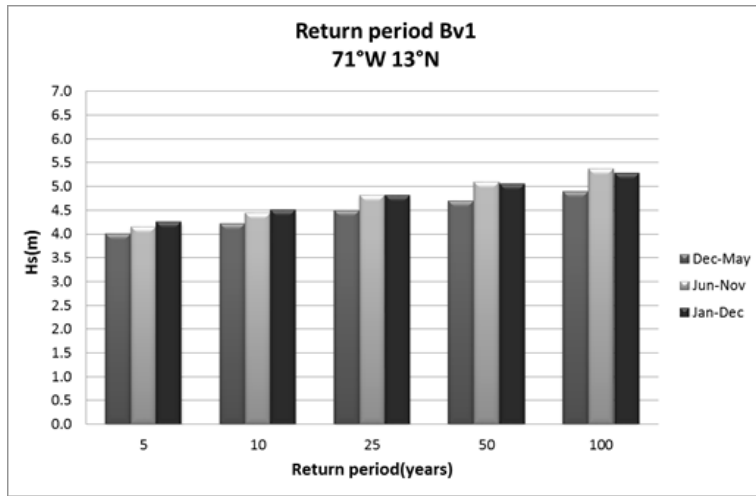
Figure 3. Scalar calibration using power and linear regression models of Hs WW3 with coinciding data from the Central Caribbean buoy (n = 594).



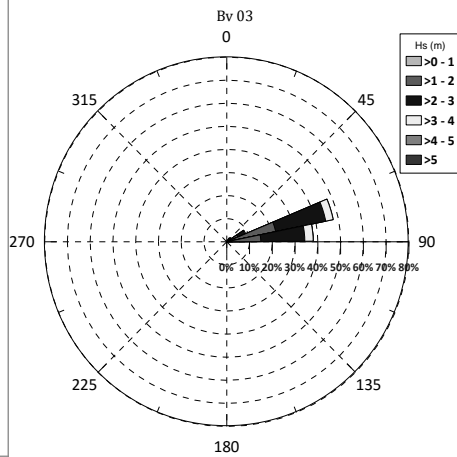
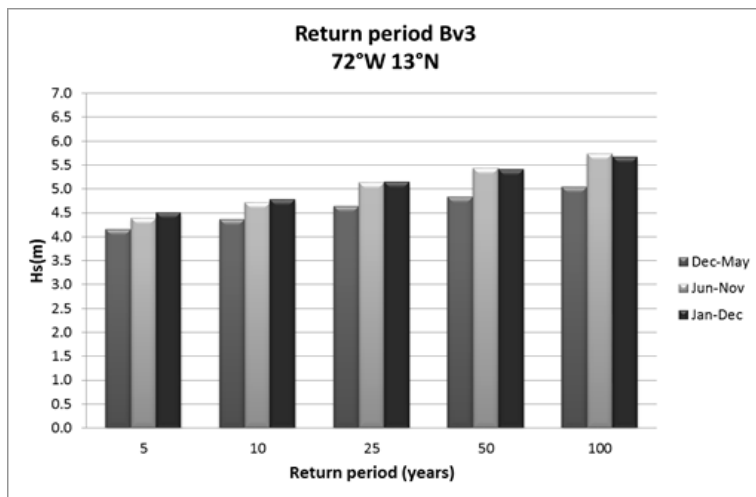
1
 2
 3 Figure 4. Validation of the H_s time series (m) corresponding to the year 2009 ($n = 767$). (4a)
 4 Buoy 41194 and WW3 data without calibration. (4b) Buoy 41194 and data corrected with the
 5 linear model. (4c) Buoy 41194 and data corrected with the power model.

6
 7
 8

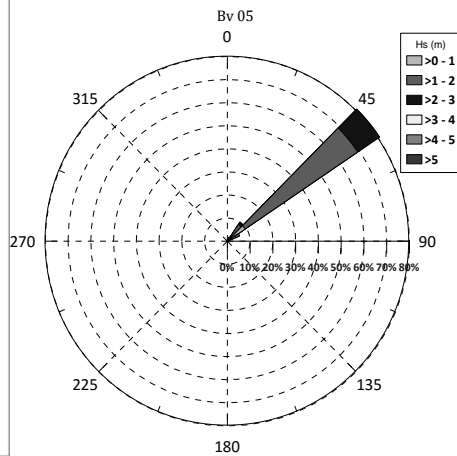
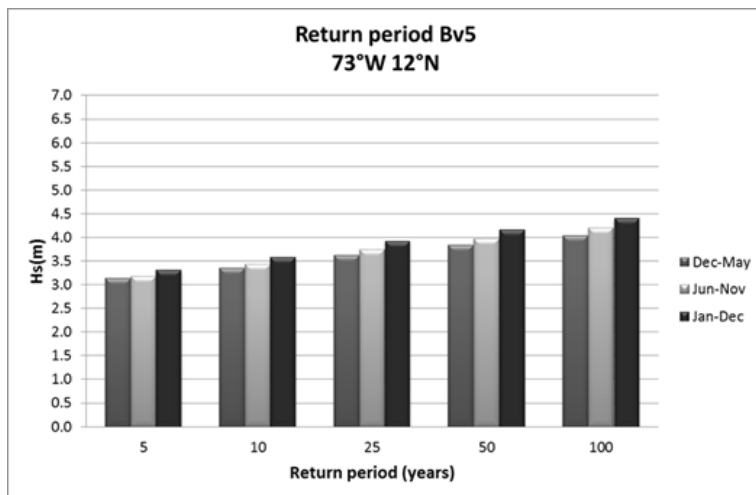
1



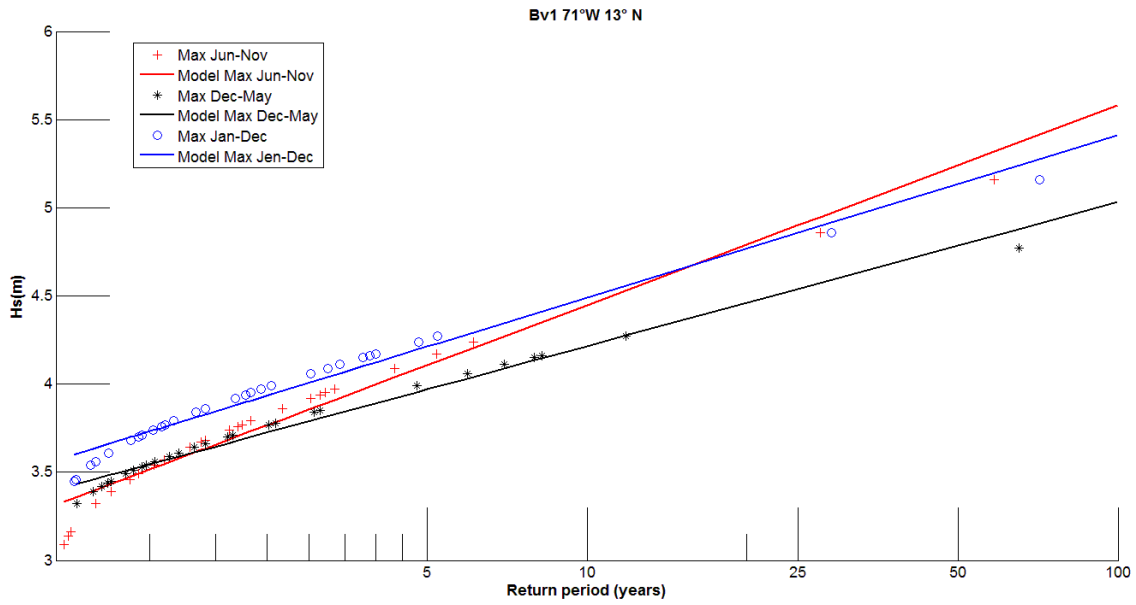
2



3

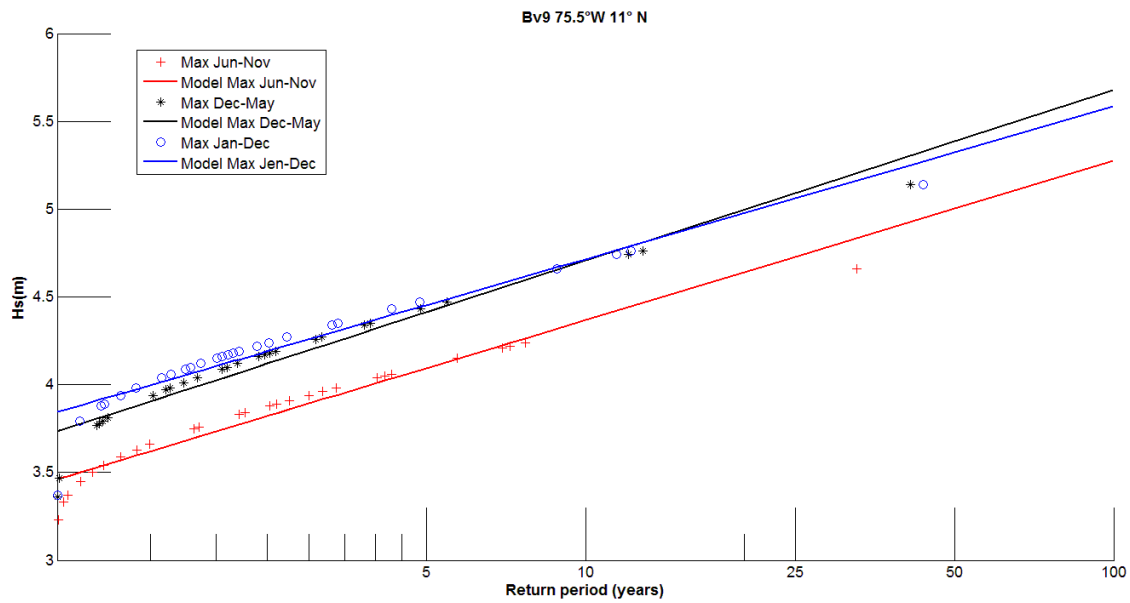


4 Figure 5. Return periods for H_s of virtual buoys BV01-BV05 (Zone 01).



1
2
3 Figure 6. Comparison of the extreme wave regime in Virtual Buoy 01, considering the
4 maximums of the complete series, the maximums of the cold front season, and the maximums of
5 the hurricane season.

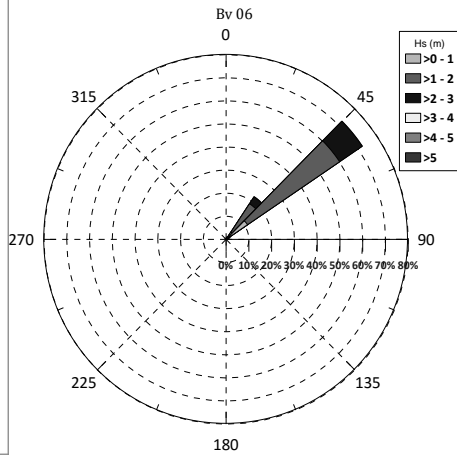
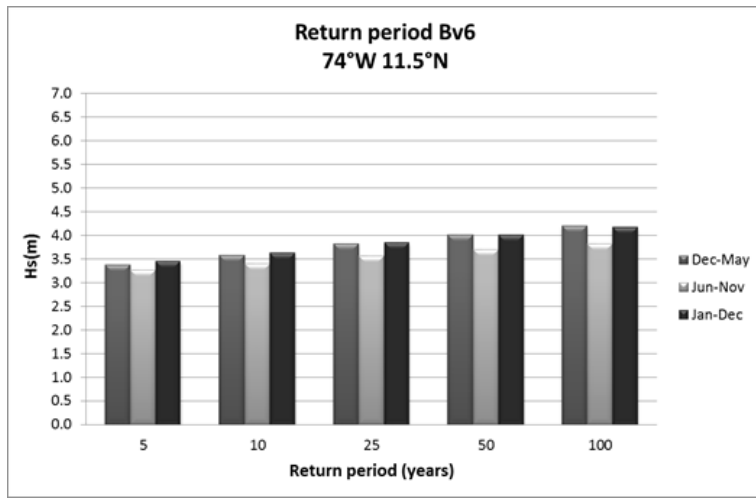
6
7
8
9
10
11
12
13
14



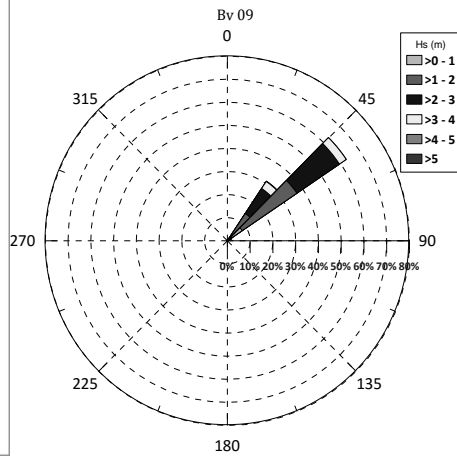
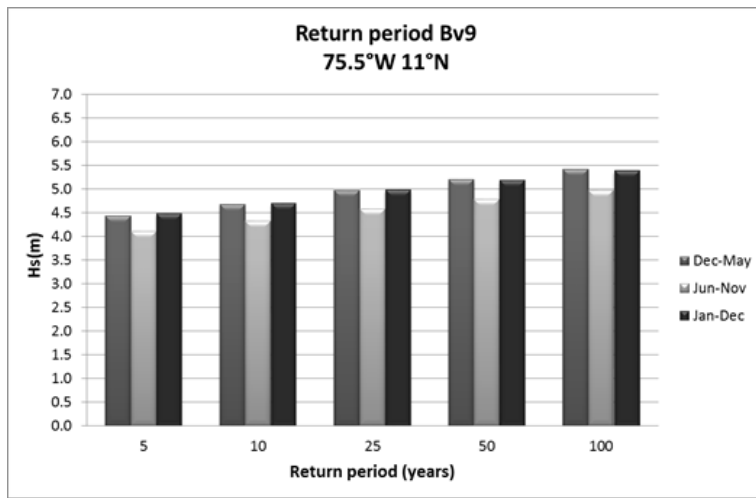
1
2
3
4
5
6
7
8
9
10
11
12

Figure 7. Comparison of the extreme wave regime in Virtual Buoy 09, considering the maximums of the complete series, the maximums of the cold front season, and the maximums of the hurricane season.

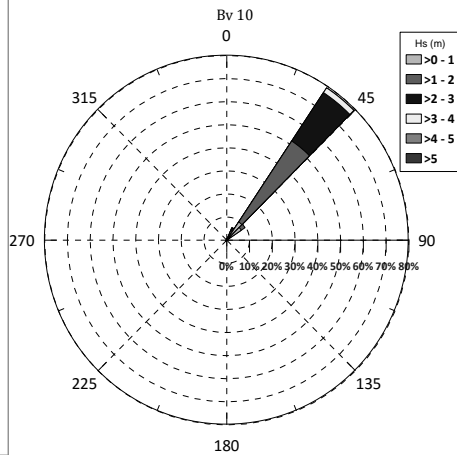
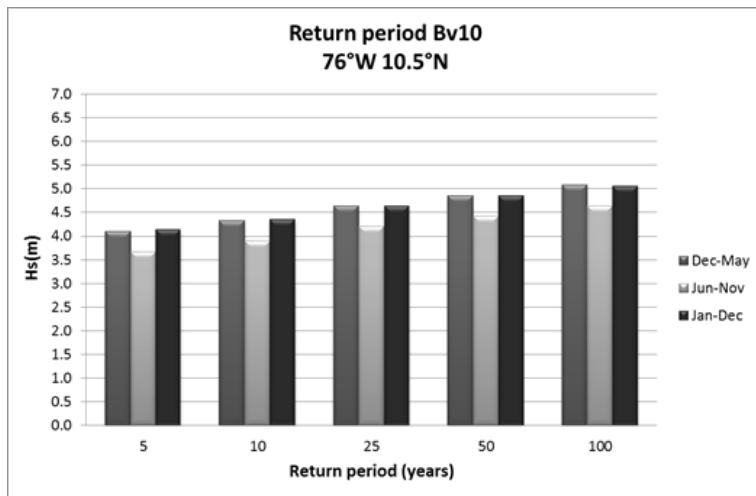
1



2



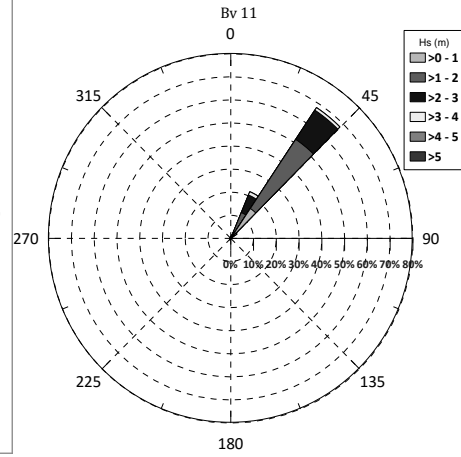
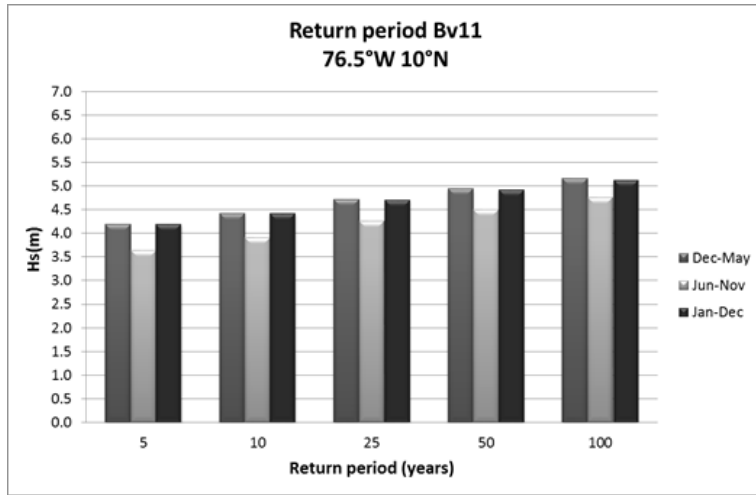
3



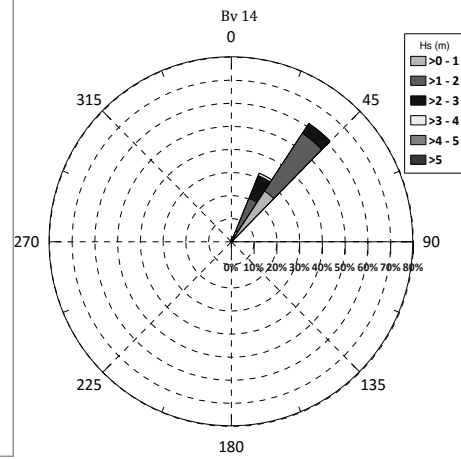
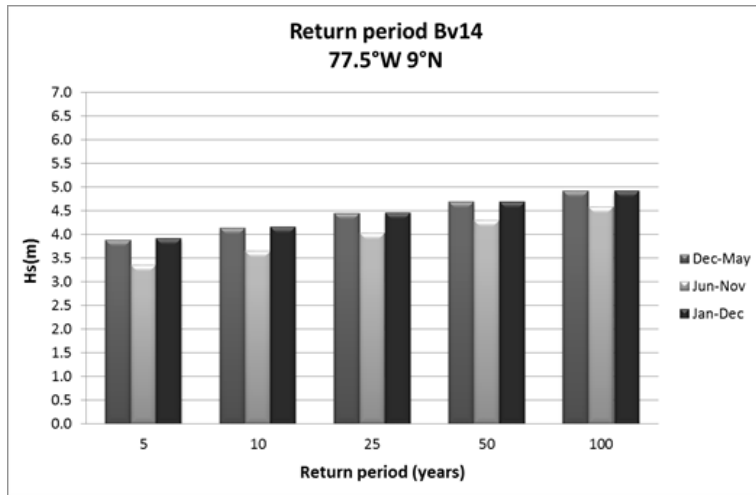
4

5 Figure 8. Return periods for Hs of virtual buoys BV6-BV10 (Zone 2).

1



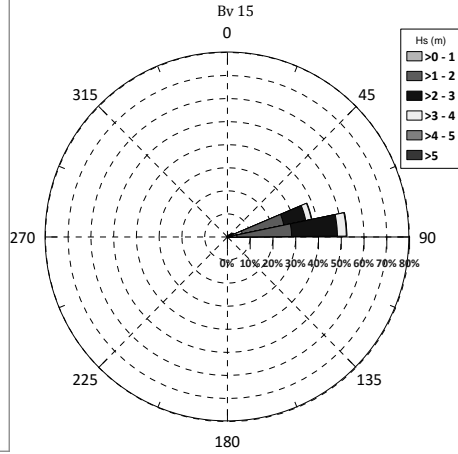
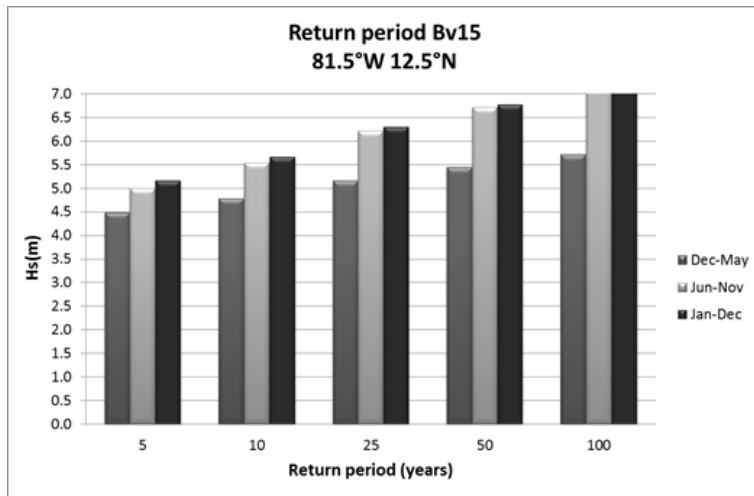
2



3

4 Figure 9. Return period for Hs of virtual buoys BV11-BV14 (Zone 03).

5



1

2

3 Figure 10. Return periods for Hs of virtual buoys BV15 (Zone 04).

4

5

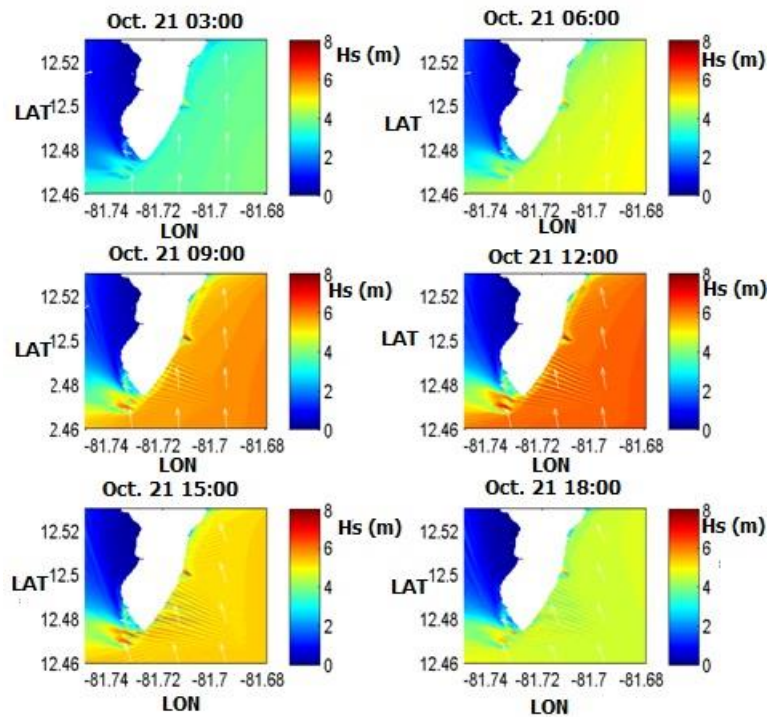
6

7

8

9

10



1
2
3
4
5
6
7

Figure 11. Significant wave height (H_s in m) fields for Hurricane Joan (1988) simulated using the SWAN model for the nested south grid in San Andres. The narrow shelf allows the energy of waves of approximately 5.0 m to affect the coastline. Source: Ortiz et al. (2014b).